Dependence of luminescence efficiency on dopant concentration and sintering temperature in the erbium-doped Ba 0.7 Sr 0.3 TiO 3 thin films

Shou-Yi Kuo, Chin-Sheng Chen, Tseung-Yuen Tseng, S.-C. Chang, and Wen-Feng Hsieh

Citation: Journal of Applied Physics **92**, 1868 (2002); doi: 10.1063/1.1492870
View online: http://dx.doi.org/10.1063/1.1492870
View Table of Contents: http://scitation.aip.org/content/aip/journal/jap/92/4?ver=pdfcov
Published by the AIP Publishing

Dependence of luminescence efficiency on dopant concentration and sintering temperature in the erbium-doped $Ba_{0.7}Sr_{0.3}TiO_3$ thin films

Shou-Yi Kuo
Institute of Electro-Optical Engineering, National Chiao Tung University, 1001 Ta-Hsueh Road, Hsinchu, Taiwan 30050, Republic of China

Chin-Sheng Chen and Tseung-Yuen Tseng
Department of Electronics Engineering and Institute of Electronics, National Chiao Tung University, 1001 Ta-Hsueh Road, Hsinchu, Taiwan 30050, Republic of China

S.-C. Chang and Wen-Feng Hsieh[a)]
Institute of Electro-Optical Engineering, National Chiao Tung University, 1001 Ta-Hsueh Road, Hsinchu, Taiwan 30050, Republic of China

(Received 22 February 2002; accepted for publication 20 May 2002)

We found the dependence of luminescence efficiency on Er^{3+} concentration and sintering temperature in the Er-doped $Ba_{0.7}Sr_{0.3}TiO_3$ (BST) thin films is governed by crystallinity and ion–ion interaction. X-ray diffraction and Raman studies of the sol-gel prepared samples show that the BST polycrystalline phase occurred when the sintering temperature reaches 700 °C, whereas, it becomes worse for temperature above 700 °C resulting from phase separation and the Er^{3+} concentration exceeding 3 mol % due to charge compensation mechanism. The observed green emission reaches maximum at sintering temperature 700 °C and 3 mol % Er^{3+} ions concentration. We also showed the Er dopant does not affect the dielectric property of BST thin films in *C–V* measurement and the $Ba_{0.7}Sr_{0.3}TiO_3$films doped with Er^{3+} ions may have potential use for electroluminescence devices.
 [DOI: 10.1063/1.1492870]

I. INTRODUCTION

Study on the luminescent properties of rare-earth (RE)-doped materials is strongly motivated because of their technological applications in photonic devices and next-generation flat-panel displays. Rare-earth ions exhibit a characteristic intra-4*f* shell luminescence which is nearly both host material and temperature independent. This feature can be used to tune the emission spectra for specific applications. Thus, it is important for systematic research of the RE ions doped in different kinds of host materials with good mechanical, thermal, electrical and electro-optical properties. Recently, many Er^{3+}-doped materials have been extensively studied because of the blue ($^2H_{9/2}\rightarrow{}^4I_{15/2}$), green ($^4S_{3/2}$,$^2H_{11/2}\rightarrow{}^4I_{15/2}$) and red ($^4F_{9/2}\rightarrow{}^4I_{15/2}$) upconversion emissions and the laser actions having been realized in a variety of glasses and fluoride crystals.[1–4] In comparison with the previously mentioned materials, barium strontium titanate is a dielectric material with excellent dielectric properties such as high dielectric constant, small dielectric loss, low leakage current, and large dielectric breakdown strength. Therefore, it is a good candidate for a RE doped host material.

Thin films of the high dielectric material $Ba_{0.7}Sr_{0.3}TiO_3$ (BST) have been intensively studied in recent years of applications in high density dynamic random access memories (DRAMs), monolithic microwave integrated circuit used for decoupling capacitors, tunable microwave filters, and phased array antennas.[5–17] The high dielectric constant of BST offers the potential of producing denser memories with simpler capacitor structures than those fabricated with conventional silicon dioxide or silicon nitride dielectrics. Combining with the merits of electricity, BST:Er will be a promising candidate for optoelectronic devices.

BST thin films have been fabricated using various methods, including metalorganic chemical vapor deposition (MOCVD),[18] rf sputtering,[19] thermal evaporation,[20] MBE,[21] and laser ablation.[22] Among those, sputtering and laser ablation are the most widely used. However, there are still some difficulties in using these processes to fabricate homogeneous films on large substrates (more than 50 mm in diameter). Due to the variation in composition and thickness the quality of films is often degraded. In contrast, the sol-gel process has the advantage of large area deposition, in addition to its low cost and convenience process control.[23]

In this article, we report the effect of Er concentration with sintering temperature on photoluminescence (PL) properties in sol-gel derived Er-doped $Ba_{0.7}Sr_{0.3}TiO_3$ (BST:Er) thin films and discuss the mechanism of emission quenching.

II. EXPERIMENT

The starting materials used for sol-gel processes were barium acetate, strontium acetate, titanium isopropoxide, and erbium acetate. Acetic acid and ethylene glycol were used as solvents. Formamide was selected as an additive to adjust the solution viscosity in order to reduce the cracks of BST thin films. $Ba(CH_3COO)_2$ and $Sr(CH_3COO)_2$ with molar ratio of 7:3 and proper amount of erbium acetate were fits dissolved

[a)]Author to whom correspondence should be addressed; electronic mail: wfhsieh@cc.nctu.edu.tw

in heated glacial acetic acid. After these starting materials were completely dissolved in heated glacial acetic acid, ethylene glycol was added into the solution and a condensation reaction occurred. Then a stoichiometric amount of Ti-isopropoxide was added into solution. Finally, formamide was added to adjust the viscosity of BST:Er precursor solution. The BST:Er precursor solution was clear and transparent.

The BST:Er precursor solution was spin coated on the $Pt/TiO_2/SiO_2/Si$ substrates and silicon substrates at 3000 rev./min for 30 s. After each spin coating, the samples were heated at 200 °C for 10 min to dry the gel and then pyrolyzed at 500 °C for 30 min in furnace. A suitable heating rate was used to avoid cracking of the BST films. Thicker films can be obtained by repeating the spin-coating process. Finally the samples were sintered at different temperature. All the sintered samples were studied by x-ray diffraction, Raman, and photoluminescence spectroscopy.

X-ray diffraction patterns (XRD) were carried out to examine the structure of the films by using a Siemens D5005 diffractometer (Cu target with a working voltage of 40 kV and current of 40 mA) in a scanning rate of 4°/min. For photoluminescence (PL) and Raman measurements, the 488 nm line of an Ar^+ laser was used as the excitation source. The emission was then analyzed using a SPEX 1877C triple grating spectrograph equipped with a cooled CCD at 140 °K. A Pt top electrode was deposited by rf sputtering for a metal/insulator/metal (MIM) structure to perform the C–V measurement. Capacitance–voltage analyses were performed at a frequency of 100 kHz using an HP8142 impedance analyzer.

III. RESULTS AND DISCUSSION

The crystalline nature of the films was identified by x-ray diffraction (XRD). Figure 1(a) shows the XRD patterns of 200-μm-thick two-layer films on $Pt/TiO_2/SiO_2/Si$ at various sintering temperatures 600–800 °C. The BST:Er thin films sintered at 600 °C show weak perovskite phase with (100), (110), and (200) orientations. Meanwhile, the secondary phases Er_2O_3 and $(Ba,Sr)_2Ti_2O_5CO_3$ were also found from XRD at 35°, 42°, and 27° indicated in Fig. 1(a), respectively.[24,25] As the sintering temperature is increased to 700 °C, the peaks of the XRD patterns become sharper and more intense, indicating better crystallinity and larger grain size. The 700 °C sintered films possess good perovskite crystallinity without the existence of second phase and are consistent with the previous report.[24,25] However, when the sintering temperature is above 750 °C, the diffraction lines at 27.5° and 29° due to $Er_2Si_2O_7$ consistent with the JCPDS data were recognized. It is believed that $Er_2Si_2O_7$phase appeared at the interface between BST:Er thin films and silicon substrate during the process of the high temperature sintering.[26] In addition, the minor line at 31° that has been ascribed to $Er_2Ti_2O_7$phase was observed as well.[27,28] We show the XRD patterns of BST films doped with various Er concentrations sintered at 700 °C in Fig. 1(b). It indicates that the BST thin film doped with Er 1 mol % has the best crystallinity and the largest grain size (57 nm) and the grain size decreases to 28 nm while the Er concentration increases

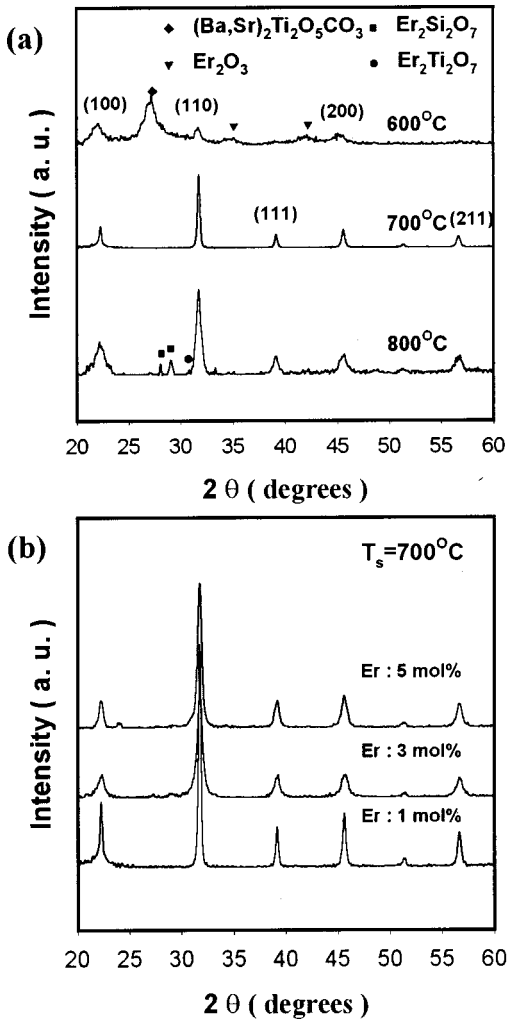

FIG. 1. XRD patterns of BST:Er thin films sintered at various temperatures (a) and doped with various Er concentrations at sintering temperature 700 °C (b).

to 5 mol %. The origin of the worst crystallinity was attributed to the Er^{3+} substitution for Ba^{2+}, which will be discussed later.

The Raman spectra of BST:Er films with various Er concentration sintered at 700 °C are plotted in Fig. 2(a). We found a broad band centered at 260 cm^{-1} corresponds to $A_1(TO_2)$ phonon mode, the 300 cm^{-1} peak is attributed to the B_1 and E(TO+LO) modes, and the asymmetric broad band near 520 cm^{-1} corresponds to E(TO) and $A_1(TO_3)$ modes.[29] A comparison of these Raman modes with various Er doping shows the increase of FWHM for the higher Er concentration. It indicates the higher Er concentration is the worse crystallinity, which is consistent with the XRD results. The appearance of sharp Raman peak at 300 cm^{-1} is a signature of the tetragonal phase $Ba_xSr_{1-x}TiO_3$ polycrystalline as described in Ref. 30. This specific Raman mode becomes broadened and weakened while phase transition from the tetragonal to cubic occurs. It is known that one can control the Curie temperature T_C of bulk $Ba_xSr_{1-x}TiO_3$ by adjusting the ratio of Ba/(Ba+Sr) by an approximate relation: $T_C(K) = 360x + 40$,[31] of which a structural change from centrosymmetric cubic to noncentrosymmetric tetragonal phase at room

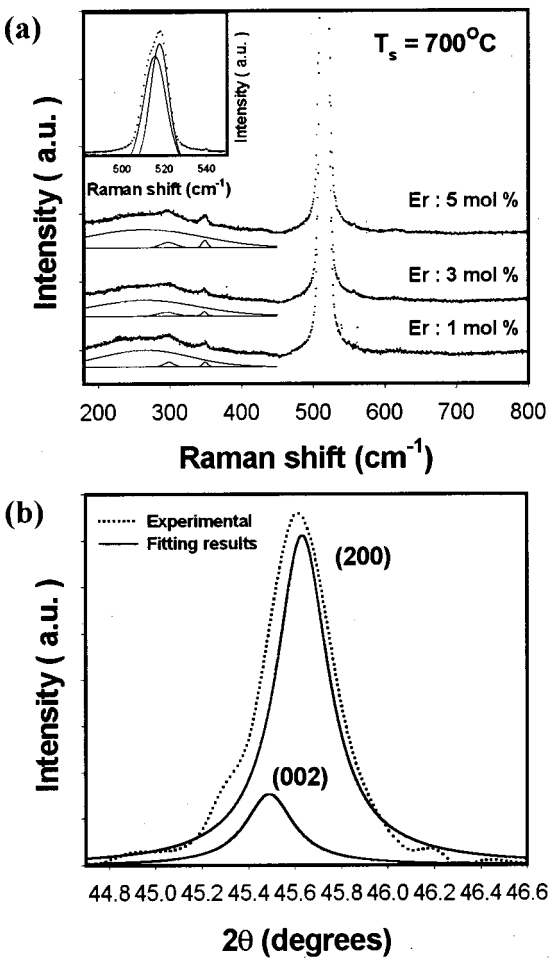

FIG. 2. Raman spectra of BST thin films doped with various Er concentrations at sintering temperature 700 °C (a) and typical expanded XRD data around 45.5° (b). The dotted and solid lines represent the experimental and fitting results, respectively.

temperature when $x \sim 0.75$. Because it has been reported that the Curie temperature of $BaTiO_3$ film is much higher than the bulk,[32] our $Ba_{0.7}Sr_{0.3}TiO_3$ films should belong to the tetragonal rather than the cubic phase that is confirmed by the expanded XRD data around 45.5° shown in Fig. 2(b).

The 3 mol % Er ions doped BST thin films sintered at 600, 700, and 800 °C show dielectric constants (ϵ) of around 230, 320, and 440 as shown in Fig. 3. The dielectric constant raised with increasing sintering temperature which is consistent with the previous report.[33] Hence, the addition of the Er dopant in this range did not affect the dielectric constant, characteristics of a good capacitor for BST.

The mechanism of emission of Er^{3+}-contained materials has been well established in the literature[34,35] and the energy diagram is schematically shown in Fig. 4. The PL spectra of $Ba_{0.7}Sr_{0.3}TiO_3$ films doped with 3 mol % of Er are shown in Fig. 5 for sintering temperatures at 600, 700, 800, and 900 °C under the 488-nm-laser excitation at room temperature. Since the host material has tetragonal rather than cubic structure, the transition selection rules of the Er ions are relaxed and the Er-related emission can be observed. The green peaks at 530 and 550 nm are attributed to the Er^{3+} inner shell $4f$ $^2H_{11/2}$ and $^4S_{3/2}$ to the $^{15}I_{15/2}$ ground level, respectively, and the weak red emission centered at 600 nm is ascribed to the $^4F_{9/2} \rightarrow {}^{15}I_{15/2}$.

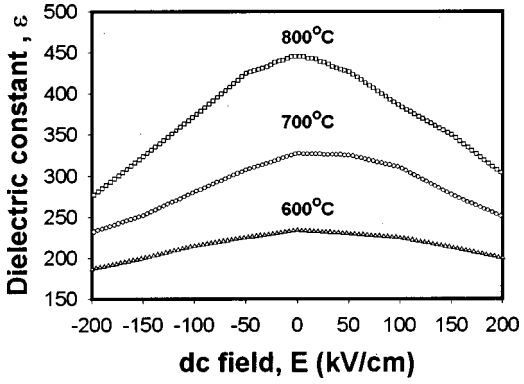

FIG. 3. ϵ–E plot of the BST:Er film capacitors sintered at 600, 700, and 800 °C.

Obviously, the shapes of the PL spectra seem quite different for the films sintered at various temperatures. There are only few broad peaks in the main emission wavelength for the film sintered at 600 °C. On the other hand, the peaks become sharper and split into several fine peaks when the films are sintered above 750 °C. The characteristic emission peaks in these films were attributed to the Stark splitting of the degenerate $4f$ levels under the crystalline field, and homogeneous and inhomogeneous broadening caused by the film's texture structures and multidomain structures. This is consistent with the XRD analysis in which the samples sintered at 600 °C indicated amorphous or weak perovskite phase and polycrystalline phase while increasing the sintering temperature.

In order to compare the relationship between the green emission and the crystallinity, shown in Fig. 6 are the PL intensities of 600, 700, 800, and 900 °C. For all the Er doping, the green emission at 550 nm reaches its maximum at

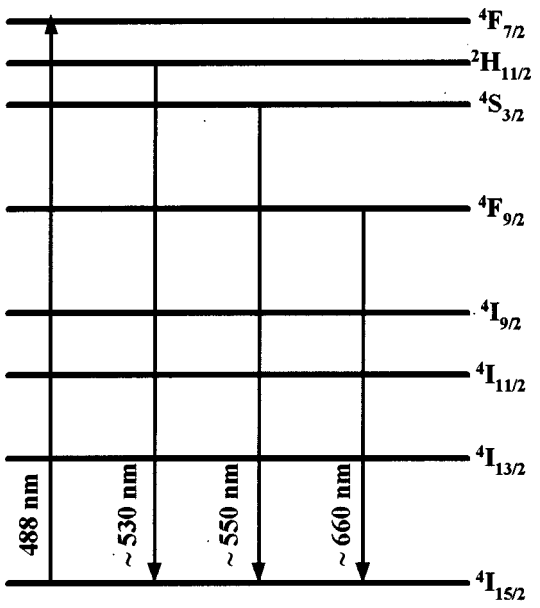

FIG. 4. Relevant energy levels in the PL of BST:Er thin films: excitation laser photon wavelength (488 nm) and Er^{3+} $4f$ energy levels.

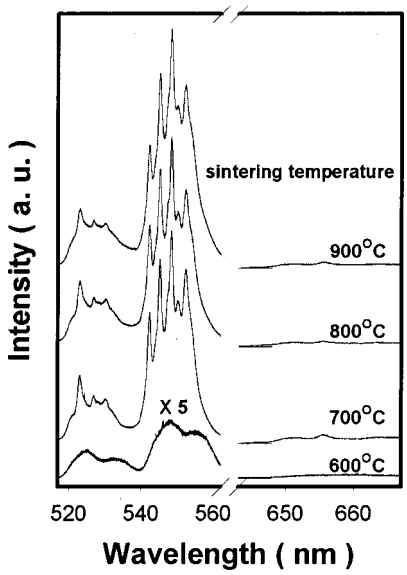

FIG. 5. Room temperature photoluminescence spectra from BST thin films doped with 3 mol % of Er under various sintering temperatures.

700 °C and is partially quenched when the samples are sintered at temperature above and below 700 °C. The diversity of emission behavior related to Er^{3+} concentration of thin films sintered at various temperatures is apparent. The quenching of the green emission which occurred in the BST:Er films is directly related to microstructural changes caused by the crystallinity, which will be discussed in detail.

From the XRD data as shown in Fig. 1(a), we have concluded that only weak crystalline phases were found in the films sintered at 600 °C and the crystallization occurred at 700 °C but formation of $Er_2Si_2O_7$ and $Er_2Ti_2O_7$ phases form above this temperature. Now, we concentrate on the influence of sintering temperature upon emission intensities. When the films belong to the weak crystalline phase sintered at 600 °C, the luminescence efficiency is low due to high defect density. The green emission reaches maximum at sintering temperature 700 °C indicates that the improvement of the crystallinity will enhance the luminescence efficiency, whereas the emission intensities decrease while the sintering temperature is above 700 °C. The quenching of the emission intensity may arise from the formation of other phases. Not only the complex compounds, e.g., Er_2O_3, $(Ba,Sr)_2Ti_2O_5CO_3$, $Er_2Si_2O_7$, and $Er_2Si_2O_7$ suppress the luminescence efficiency due to optical scattering or absorption, but the Er_2O_3 has cubic symmetry as well. While the Er ions occupy the centrosymmetry position of Er_2O_3 crystal, the $^4S_{3/2} \rightarrow {}^4I_{15/2}$ transition is forbidden and therefore would reduce luminescence efficiency.

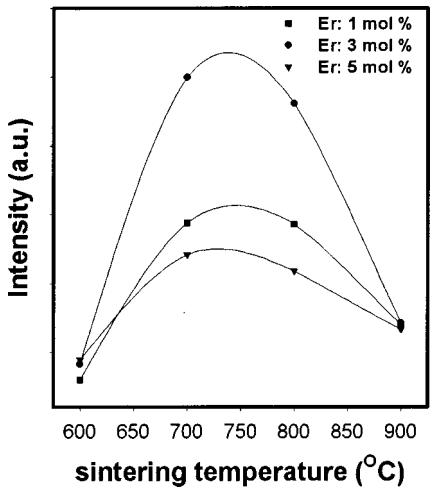

FIG. 6. Dependence of the green emission intensities of BST:Er thin films on Er concentration and sintering temperature.

For studying the effect of Er^{3+} concentration on emission intensity of the BST:Er films, we found as shown in Fig. 6 the emission intensities increase with increasing Er^{3+} concentration for 600 °C sintered BST:Er films which have the weak crystalline phase. The doped Er^{3+} ions in the weak crystalline phase are dissolvable. A noticeable difference contrast to the films in weak crystalline phase was observed while the BST:Er thin films belong to polycrystalline phase, sintered at 700, 800, and 900 °C. It can be clearly seen that the emission intensities of the BST:Er films increase as the Er doping concentration increases from 1 to 3 mol %. Meanwhile, the PL intensity diminishes as Er doping concentration exceed 3 mol %.

The quenching mechanism is thought to be a cross-relaxation process between two closely placed Er^{3+} ions. In this experiment, the ion density N of 1, 3, and 5 mol % Er doping is 1.5×10^{20}, 4.5×10^{20}, and $7.5\times10^{20}/cm^3$, respectively. Ion pairs and clusters can be formed easily in the $Ba_{0.7}Sr_{0.3}TiO_3$ lattice.[36,37] The Er^{3+} ion is likely to take the position of the Ba^{2+} or Sr^{2+} due to similar ionic radius. The substitution of Er^{3+} for the nearest Ti^{4+} ion in the oxygen octahedron is difficult because of large difference in size between Er^{3+} and Ti^{4+}. To maintain electrical neutrality, one approach is to replace the nearest Ba^{2+} ion by another Er^{3+} ion with, additionally, the formation of a Ba vacancy. As shown in Figs. 1(b) and 2(a), the increase of Er^{3+} concentration from 1 to 5 mol % results in the worse crystallinity. From charge compensation mechanism, the smallest $Er^{3+}-Er^{3+}$ distance is about 0.4–0.5 nm in $Ba_{0.7}Sr_{0.3}TiO_3$ lattice and cross relaxation is greatly enhanced, resulting in decrease in luminescence intensity. Very efficient cross relaxation can occur when two or more Er ions sit close to one another to form a cluster that results in almost immediate interaction between the ions.[38] The interaction strength is very sensitive to the change in γ, which is the distance between two Er^{3+} ions, and is found to be proportional to $1/\gamma^m$ ($m=6$, 8, and 10).[2] In our $Ba_{0.7}Sr_{0.3}TiO_3$ thin films doped with 1, 3, and 5 mol % Er, the mean distance between Er^{3+} ions is estimated by $\gamma=0.62\times N^{-1/3}$,[39] corresponding to $\gamma=1.2$, 0.81, and 0.68 nm. It is very likely the mean distance of 0.68 nm of 5 mol % BST:Er will increase the probability of Er^{3+} ions sitting at the nearest-neighbor positions. Not only slightly structural damage was found from XRD and Raman measurement, but also enhanced luminescence quenching was observed. Consequently, the emission intensity diminishes while the Er concentration exceed 3 mol %.

IV. CONCLUSION

The BST:Er films prepared by sol-gel technique under various sintering temperatures have been studied by XRD, *C–V*, Raman, and PL measurements. We found that the BST:Er films belong to weak crystalline phase sintered at 600 °C and polycrystalline phase sintered above 700 °C. The addition of Er dopant does not downgrade the electronic property of barium–strontimum titanate. The emission efficiency of BST:Er thin films was found to be dominated by the mean distance between Er^{3+} ions and solubility of Er^{3+} in polycrystalline and weak crystalline phase. The emission intensities of the films reach maximum at 3 mol % Er ions dopant concentration and sintering temperature 700 °C. The presence of clusters for the Er concentration exceed 3 mol % will diminishes the emission intensity. Moreover, the improvement of the crystallinity of BST:Er films enhances the green emission enhancement. Good performance on both electric and optical properties of the BST:Er thin films show potential applications in photonic devices.

[1] J. Heikenfeld, M. Garter, D. S. Lee, R. Birkhahn, and A. J. Steckl, Appl. Phys. Lett. **75**, 1189 (1999).
[2] H. X. Zhang, C. H. Kam, Y. Zhou, X. Q. Han, S. Buddhudu, Q. Xiang, Y. L. Lam, and Y. C. Chan, Appl. Phys. Lett. **77**, 609 (2000).
[3] S. M. Takahashi, M. Kanno, and R. Kawamoto, Appl. Phys. Lett. **65**, 1874 (1994).
[4] J. Heikenfeld, D. S. Lee, M. Garter, R. Birkhahn, and A. J. Steckl, Appl. Phys. Lett. **76**, 1365 (2000).
[5] R. Liedtke, M. Grossmann, and R. Waser, Appl. Phys. Lett. **77**, 2045 (2000).
[6] N. A. Pertsev, V. G. Koukhar, R. Waser, and S. Hoffmann, Appl. Phys. Lett. **77**, 2596 (2000).
[7] J. Im, S. K. Streiffer, O. Auciello, and A. R. Krauss, Appl. Phys. Lett. **77**, 2593 (2000).
[8] S. M. Rhim, H. Bak, S. Hong, and O. K. Kim, J. Am. Ceram. Soc. **83**, 3009 (2000).
[9] A. I. Kingon, J. P. Maria, and S. K. Streiffer, Nature (London) **406**, 1032 (2000).
[10] D. E. Kotecki, J. D. Baniecki, H. Shen, R. B. Laibowitz, K. L. Saenger, J. J. Lian, T. M. Shaw, S. D. Athavale, C. Cabral, P. R. Duncombe, M. Gutsche, G. Kunkel, Y. J. Park, Y. Y. Wang, and R. Wise, IBM J. Res. Dev. **43**, 367 (1999).
[11] J. D. Baniecki, R. B. Laibowitz, T. M. Shaw, K. L. Saenger, P. R. Duncombe, C. Cabral, D. E. Kotecki, H. Shen, J. Lian, and Q. Y. Ma, J. Eur. Ceram. Soc. **19**, 1457 (1999).
[12] C. S. Hwang, B. T. Lee, C. S. Kang, K. H. Lee, H. J. Cho, H. Hideki, W. D. Kim, S. I. Lee, and M. Y. Lee, J. Appl. Phys. **85**, 287 (1999).
[13] J. D. Baniecki, R. B. Laibowitz, T. M. Shaw, P. R. Duncombe, D. A. Neumayer, D. E. Kotecki, H. Shen, and Q. Y. Ma, Appl. Phys. Lett. **72**, 498 (1998).
[14] G. W. Dietz, M. Schumacher, R. Waser, S. K. Streiffer, C. Basceri, and A. I. Kingon, J. Appl. Phys. **82**, 2359 (1997).
[15] C. Basceri, S. K. Streiffer, A. I. Kingon, and R. Waser, J. Appl. Phys. **82**, 2497 (1997).
[16] G. T. Stauf, C. Ragaglia, J. F. Roeder, D. Vestyck, J. P. Maria, T. Ayguavives, A. Kingon, A. Mortazawi, and A. Tombak, Integr. Ferroelectr. **39**, 1271 (2001).
[17] S. C. Tidrow, E. Adler, T. Anthony, W. Wiebach, and J. Synowczynski, Integr. Ferroelectr. **29**, 151 (2000).
[18] B. S. Kwak, K. Zhang, E. P. Boyd, A. Erbil, and B. J. Wilkens, J. Appl. Phys. **69**, 767 (1991).
[19] S. Kim, S. Hishita, Y. M. Kang, and S. Baik, J. Appl. Phys. **78**, 5604 (1995).
[20] K. Iijima, T. Terashima, K. Yamamoto, K. Hirata, and Y. Bando, Appl. Phys. Lett. **56**, 527 (1990).
[21] R. A. McKee, F. J. Walker, J. R. Conner, E. D. Specht, and D. E. Zelmon, Appl. Phys. Lett. **59**, 782 (1991).
[22] K. Nashimoto, D. K. Fork, F. A. Ponce, and J. C. Tramontana, Jpn. J. Appl. Phys., Part 1 **32**, 4099 (1993).
[23] F. Wang, A. Uusimaki, S. Leppavuori, S. F. Karmanenko, A. I. Dedyk, V. I. Sakharov, and I. T. Serenkov, J. Mater. Res. **13**, 1243 (1998).
[24] C. L. Jia, K. Urban, S. Hoffmann, and R. Waser, J. Mater. Res. **13**, 2206 (1998).
[25] S. Hoffmann and R. Waser, J. Eur. Ceram. Soc. **19**, 1339 (1999).
[26] K. Hafidi, Y. Idjiyaou, M. Azizan, E. L. Ameziane, A. Outzourhit, T. A. Nguyen Tan, and M. Brunel, Appl. Surf. Sci. **108**, 251 (1997).
[27] J. H. Hwang, S. K. Choi, and Y. H. Han, Jpn. J. Appl. Phys., Part 1 **40**, 4952 (2001).
[28] J. H. Hwang and Y. H. Han, Jpn. J. Appl. Phys., Part 1 **40**, 676 (2001).
[29] M. DiDomenico, S. H. Wemple, and S. P. Porto, Phys. Rev. **174**, 524 (1968).
[30] R. Naik, J. J. Nazarko, C. S. Flattery, U. D. Venkateswaran, V. M. Naik, M. S. Mohammed, G. W. Auner, J. V. Mantese, N. W. Schubring, A. L. Micheli, and A. B. Catalan, Phys. Rev. B **61**, 11 367 (2000).
[31] S. Y. Kuo, W. Y. Liao, and W. F. Hsieh, Phys. Rev. B **64**, 224103 (2001).
[32] C. L. Li, Z. H. Chen, Y. L. Zhou, H. B. Lu, C. Dong, F. Wu, and H. Chen, J. Appl. Phys. **86**, 4555 (1999).
[33] S. Ezhilvalavan and T. Y. Tseng, Mater. Chem. Phys. **65**, 227 (2000).
[34] C. H. Huang and L. McCaughan, IEEE Photonics Technol. Lett. **9**, 599 (1997).
[35] K. W. Kramer, H. U. Gudel, and R. N. Schwartz, Phys. Rev. B **56**, 13 830 (1997).
[36] F. Goutaland, Y. Ouerdane, A. Boukenter, and G. Monnom, J. Alloys Compd. **275-277**, 276 (1998).
[37] J. Zheng, Y. Lu, X. Chen, M. C. Golomb, and J. Zhao, Appl. Phys. Lett. **75**, 3470 (1999).
[38] W. J. Minscalco, J. Lightwave Technol. **9**, 234 (1991).
[39] C. Y. Chen, R. R. Petrin, D. C. Yeh, W. A. Sibley, and J. L. Adam, Opt. Lett. **14**, 432 (1989).